

LETTER

Linear cavity fiber laser harmonically mode-locked with SESAM

To cite this article: D A Stoliarov *et al* 2020 *Laser Phys. Lett.* **17** 105102

View the [article online](#) for updates and enhancements.



IOP | ebooks™

Bringing together innovative digital publishing with leading authors from the global scientific community.

Start exploring the collection—download the first chapter of every title for free.

Letter

Linear cavity fiber laser harmonically mode-locked with SESAM

D A Stoliarov, P A Itrin, V A Ribenek, D A Korobko and A A Fotiadi

Ulyanovsk State University, 42 Leo Tolstoy Street, Ulyanovsk 432017, Russia

E-mail: korobkotam@rambler.ru

Received 3 April 2020

Accepted for publication 31 July 2020

Published 10 September 2020

**Abstract**

A linear cavity picosecond Er-fiber laser, which was passively and harmonically mode-locked with SESAM, is demonstrated. The advantage of the proposed configuration is the fast tuning of the pulse repetition rate in the range from tens of MHz to 1 GHz, realized by varying the pump power without any additional adjustment of the polarization.

Keywords: fiber lasers, harmonic mode-locking, linear cavity

(Some figures may appear in colour only in the online journal)

1. Introduction

Laser sources of high-repetition-rate pulse trains have widespread photonic applications. For example, in the fields of fiber communications, spectroscopy, frequency comb generation, etc [1, 2]. Among them, harmonically mode-locked (HML) soliton fiber lasers exhibiting advantageous consumer properties, such as compactness, reliability, low cost and maintaining convenient output, are mostly demanded [3, 4].

Recent progress in the development of fiber HML lasers has been achieved due to different special techniques. Restricting ourselves to only passive HML schemes, the intensive development of a fiber ring laser with an intracavity filter could be distinguished. The particular feature of these sources consisting in the absence of a special saturable absorber makes them rather attractive for some applications [5, 6]. However, to get the GHz pulse repetition rates the Q-factor of the intracavity filter should be able to select individual modes from hundreds or thousands of laser cavity modes [7]. Another disadvantage of this method is the requirement of complex stabilization setups to synchronize the free spectral range (FSR) of the filter with the FSR of the ring fiber cavity [8]. The ring fiber cavities are also applied in traditional configurations of HML lasers used for the passive mode-locking nonlinear polarization rotation (NPR) technique [9, 10] or for saturable absorbers based on graphene or carbon nanotubes [11, 12].

In this work, a harmonic mode-locking scheme utilizing linear fiber cavity is considered. It is known that NPR mode-locking is impossible in a linear cavity so other mode-locking mechanisms should be used in this case. As a result, such lasers do not require periodic polarization adjusting that facilitates their self-starting and increases stability. Fundamentally mode-locked linear cavity fiber lasers with high pulse repetition rates (\sim GHz) are known [13, 14]. Their obvious disadvantages arising from their short cavity (\sim 10 cm) are a small output power, limited tuning options and high requirements for cavity components (mirrors, pump diodes, etc). Known linear cavity HML lasers using the ‘colliding pulses’ technique achieved the pulse repetition rate at hundreds of MHz [15, 16]. This scheme is similar to the ring cavity with an intracavity filter and does not allow the repetition rate tuning without a rearrangement of the cavity. As far as we know, in this work the linear cavity HML fiber laser with a rather broad tuning of the pulse repetition rate (from tens of MHz to 1 GHz) is first demonstrated.

2. Experimental setup

The considered fiber laser scheme is shown in figure 1. The linear cavity consists of a 0.6 m Er-doped fiber (EDF-150 OFC) as a gain medium that is pumped by a couple of 976 nm laser

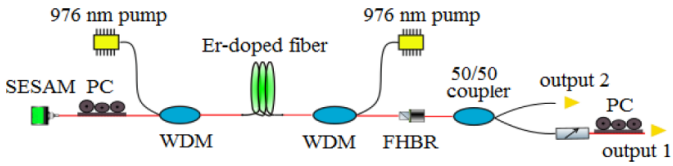


Figure 1. Experimental setup. FHBR—a fiber hybrid broadband reflector, WDM—a wavelength division multiplexer, PC—a polarization controller.

diodes with power of up to 400 mW through two 976/1550 WDMs. The cavity is terminated by a fiber hybrid broadband reflector (FHBR) from one end and by the SESAM structure from the other end. The SESAM (BATOP SAM-1550-4.0x2.0-25.0g-c) has a relaxation time of 2 ps, a modulation depth of 15% and an unsaturated loss of 10%. The transmission of the FHBR is equal to 10% with a central wavelength of $\lambda = 1550$ nm, a minimal bandwidth of 7 nm at the 0.5 dB level and stop bands at 1520 ~ 1543 and 1557 ~ 1610 nm (at the 25 dB level). All cavity elements are spliced by a standard SMF-28 fiber, so the total cavity length is $L = 3.89$ m corresponding to a fundamental frequency of 26.52 MHz. The total cavity dispersion can be estimated as the sum of the dispersions of all fiber elements. Its value is about 0.11 ps².

The experimental results were detected by a spectrum analyzer HP 70950B (resolution of 0.1 nm) and a scanning autocorrelator FR103-WS. A radiofrequency (RF) spectrum analyzer R&S FSP40 and a photodetector MACOM D-8IR were used to indicate the RF signal of the laser.

3. Results

When the pump power exceeds 22 mW, the laser self-starts in the fundamental mode-locking mode at central wavelength $\lambda_0 \sim 1553$ nm. With the increase of the pump power, the laser proceeds its operation in multiple pulse generation with a periodic pulse arrangement into the cavity, *i.e.* it demonstrates harmonic mode-locking. Increasing the pump power up to 480 mW at a certain PC orientation, we observe the generation of the pulse train with repetition rate 1060.9 MHz, which corresponds to the fortieth harmonic of the cavity. The obtained laser settings provide the harmonic mode-locking in a wide intermediate range of repetition rates (from fundamental frequency 26.5 MHz to a maximal repetition rate of 1060.9 MHz) by varying the pump power without any additional PC adjusting. Figure 2 shows the changes in the laser outputs in dependence on the pump power.

As can be seen in figure 2(a), the pulse repetition rate increases proportionally to the pump power. The changes in the output power are not in exact agreement with the linear law leading to the changes in calculated energy of the single pulse in the range from 3.5–10 pJ (figure 2(b)). As one can see, the single pulse energy increases with the repetition rate. The quality of the generated pulse train can be estimated by the oscilloscope trace and RF spectrum (figure 3). As one can see from figure 2(b), the signal to noise ratio (SNR) obtained from the high-resolution RF spectrum decreases from ~57 dB for the fundamental frequency to ~34 dB for the maximal repetition

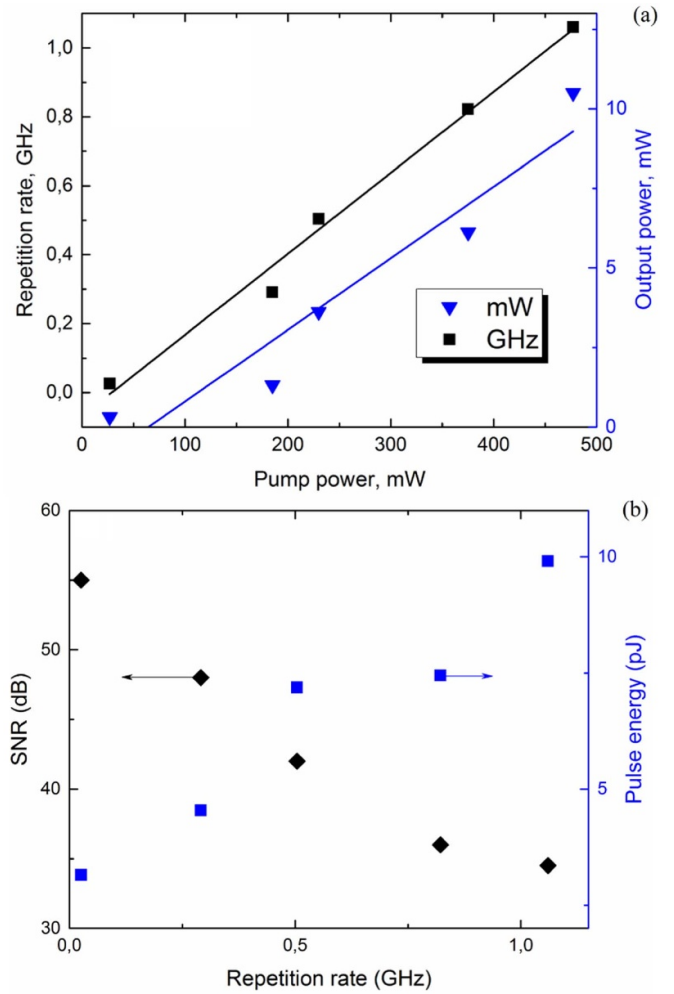


Figure 2. (a) Dependence of the pulse repetition rate and output power on the pump power. (b) Dependence of the SNR and single pulse energy on the pulse repetition rate.

rate. The example of the high-resolution RF spectrum recorded for the repetition rate of 1060.9 MHz is shown in the inset of figure 3(b). Using these data, the quantitative estimation of the corresponding pulse train low-frequency jitter can be performed as: $\Delta t/T = (1/2\pi) (\Delta P \Delta f / \Delta f_{res})^{1/2} \sim 0.05 - 0.5\%$ [17], where T is the fundamental period of the laser cavity, ΔP is the SNR, Δf is the width of the pedestal and Δf_{res} is the resolution of the spectrum analyzer (30 Hz). Figure 3(b) also shows the measured RF spectrum with a resolution of 1 kHz that allows a calculation of the side-mode suppression level. For all received pulse trains it is less than -60 dB.

As it was mentioned, the cavity possesses anomalous dispersion so the laser generates soliton pulses. The measured optical spectra and autocorrelation traces of generated pulses for the fundamental frequency and maximal repetition rate of 1060.9 MHz are demonstrated in figures 4 and 5. Note that the optical spectra of the generated pulses do not comprise specific bands typical for the cw component or dispersive waves (figures 4). The FWHM pulse spectrum width increases with the repetition rate from the value $\Delta \lambda_{FWHM} \sim 0.14$ nm for the

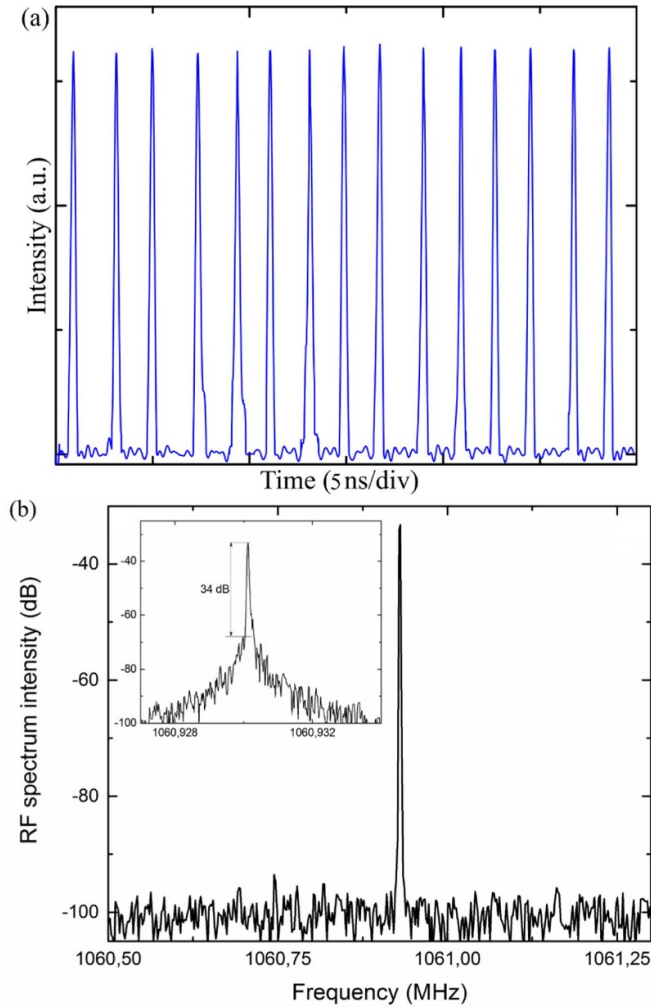


Figure 3. (a) Oscilloscope trace and (b) RF spectrum of the pulse train with repetition rate of 1060.9 MHz measured with a resolution of 1 kHz. Inset: RF spectrum measured with a resolution of 30 Hz.

fundamental frequency to the value $\Delta\lambda_{FWHM} \sim 0.24$ nm corresponding to the repetition rate of 1060.9 MHz. On the contrary, the FWHM pulse duration decreases from the maximal value of 18.3 ps for the fundamental frequency to the minimum of 10.4 ps corresponding to the repetition rate of 1060.9 MHz (figures 5). The calculated time–bandwidth product is ~ 0.32 , approving that the generated pulses are close to transform-limited solitons. As expected, higher energy pulses with the maximal repetition rate (figure 2(b)) have a minimal duration of 10.4 ps and vice-versa the duration of lower energy pulses generated at the fundamental frequency is maximal (18.3 ps). A relatively narrow spectrum width can be explained by the mismatch between the central wavelength of the FHBR ($\lambda = 1550$ nm) and the gain peak located in the region of the longer wavelengths. The resulting effective filter is strong enough to suppress the dispersion waves and the possible cw-component of radiation. We believe that the pump growth increases the bandwidth of the filter providing not only the generation of new solitons in the cavity, but also the enlargement of the single soliton energy and the broadening of its spectrum width.

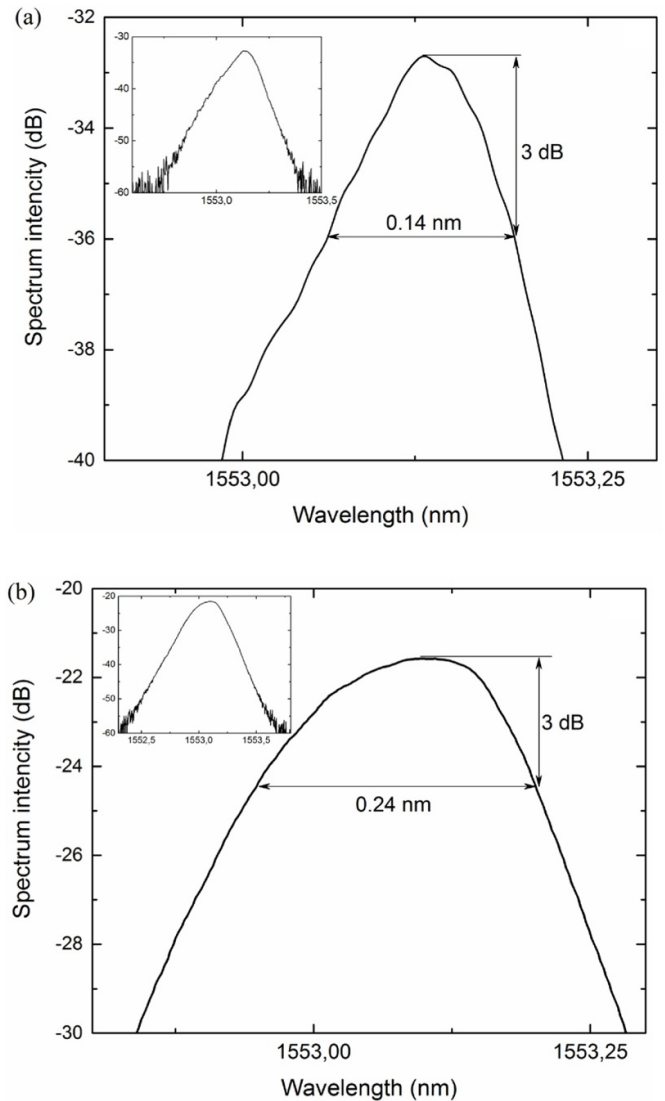


Figure 4. Optical spectra of generated pulse trains. (a) For the fundamental frequency, (b) for the repetition rate of 1060.9 MHz (40th cavity harmonic). Insets: wide span spectra.

4. Conclusions

The linear cavity Er-fiber laser HML by SESAM is demonstrated. After the initial adjustment of the PC, the laser generates trains of picosecond soliton pulses with repetition rates belonging to the range from tens of MHz to 1 GHz. Variation of the pump power leads to an automatic change in the pulse repetition rate without an additional polarization adjustment. The filtering effect arises due to a mismatch between the central wavelength of the output reflector and the gain peak leads to a rather narrow spectrum width, but also facilitates the whole suppression of dispersion waves and the radiation cw-component. The proposed experimental scheme is promising for stable optical frequency comb generation with possible tuning of the FSR, and can be applied in radiophotonics, spectroscopy, etc. The disadvantage of the method is the relatively low output pulse energy (10 pJ and less). However, the proposed laser source can easily be included in cascade

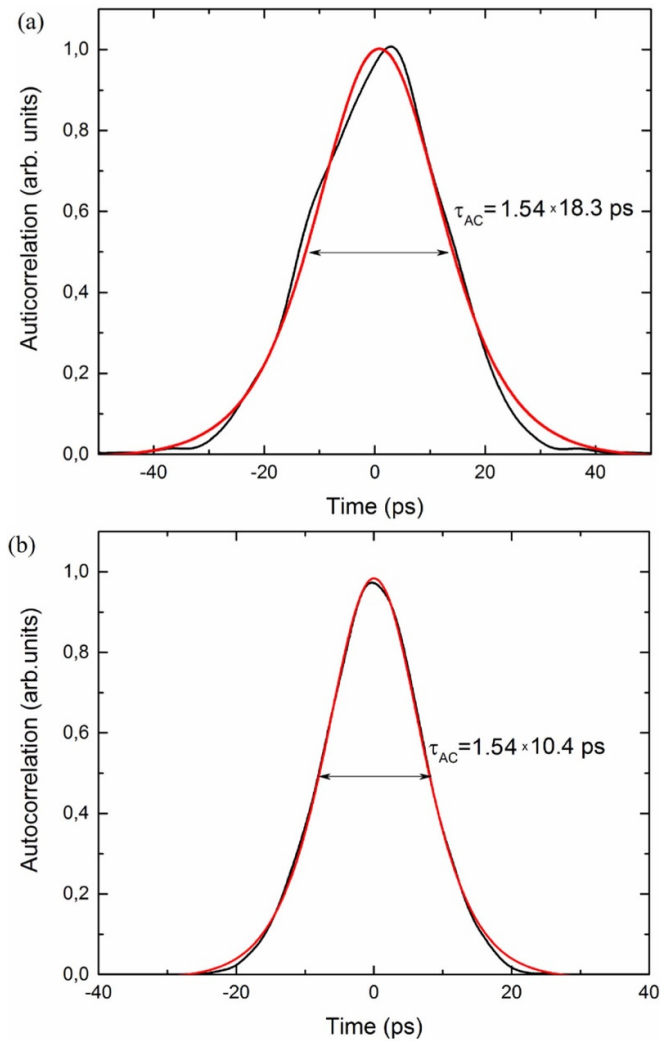


Figure 5. Autocorrelation traces of generated pulses. (a) For the pulse train with fundamental frequency, (b) for the pulse train with repetition rate of 1060.9 MHz (40th cavity harmonic).

amplifying schemes, increasing the pulse energy by orders of magnitude [18, 19].

Acknowledgments

This work was supported by the Russian Science Foundation (project #19-72-10037), the Russian Foundation for Basic Research (grant #19-42-730009) and the Russian Ministry of Science and High Education (state program 0830-2020-0009).

References

- [1] Bartels A, Heinecke D and Diddams S A 2008 *Opt. Lett.* **33** 1905
- [2] Schliesser A, Picqué N and Hänsch T W 2012 *Nat. Photonics* **6** 440
- [3] Fermann M E and Hartl I 2013 *Nat. Photonics* **7** 868
- [4] Shi W, Fang Q, Zhu X, Norwood R A and Peyghambarian N 2014 *Appl. Opt.* **53** 6554
- [5] Andrianov A V, Mylnikov V M, Koptev M Y, Muravyev S V and Kim A V 2016 *Quantum Electron.* **46** 387
- [6] Mao D, Liu X, Sun Z, Lu H, Han D, Wang G and Wang F 2013 *Sci. Rep.* **3** 3223
- [7] Korobko D A, Fotiadi A A and Zolotovskii I O 2017 *Opt. Express* **25** 21180
- [8] Sobon G, Krzempek K, Kaczmarek P, Abramski K M and Nikodem M 2011 *Opt. Commun.* **284** 4203
- [9] Lecaplain C and Grelu P 2013 *Opt. Express* **21** 10897
- [10] Trikshev A I, Kamynin V A, Tsvetkov V B and Itrin P A 2018 *Quantum Electron.* **48** 1109
- [11] Huang Q, Huang Z, Al Araiimi M, Rozhin A and Mou C 2020 *IEEE Photonics Technol. Lett.* **32** 121
- [12] Sobon G, Sotor J and Abramski K M 2012 *Appl. Phys. Lett.* **100** 161109
- [13] Ma Y, Zhu X, Yang L, Tong M, Norwood R A, Wei H and Li J 2019 *Opt. Express* **27** 14487
- [14] Cheng H, Lin W, Luo Z and Yang Z 2018 *IEEE J. Sel. Top. Quantum Electron.* **24** 1100106
- [15] Deng Y, Koch M W, Lu F, Wicks G W and Knox W H 2004 *Opt. Express* **12** 3872
- [16] Okhotnikov O G and Guina M 2001 *Appl. Phys. B* **72** 381
- [17] Von der Linde D 1986 *Appl. Phys. B* **39** 201
- [18] Kotov L, Likhachev M, Bubnov M, Medvedkov O, Lipatov D, Guryanov A and Février S 2015 *Opt. Lett.* **40** 1189
- [19] Stoliarov D A, Korobko D A, Zolotovskii I O and Sysolyatin A A 2019 *Opt. Spectrosc.* **126638**